metals

MDPI

Communication

Enhanced Absorptance of 45# Steel by Laser-Induced Periodic Surface Structures (LIPSS)

Tianyu Wang [1,2], Jintian Bian [1,2,*], Xin Li [1,2,*], Hui Kong [1,2], Lei Wang [1,2], Xi Wang [1,2] and Xiaoquan Sun [1,2,*]

[1] State Key Laboratory of Pulsed Power Laser Technology, National University of Defense Technology, 460 Huangshan Road, Hefei 230009, China; wangty1995@nudt.edu.cn (T.W.); konghui17@nudt.edu.cn (H.K.); 18326063953@163.com (L.W.); eastangus@126.com (X.W.)

[2] Anhui Key Laboratory of Advanced Laser Technology, National University of Defense Technology, 460 Huangshan Road, Hefei 230009, China

* Correspondence: bianjintian17@nudt.edu.cn (J.B.); lixinkiller@nudt.edu.cn (X.L.); sun_xq@nudt.edu.cn (X.S.); Tel.:+86-0451-65927805 (J.B.); +86-0451-65927811 (X.L.); +86-0451-65927801 (X.S.)

Received: 19 August 2020; Accepted: 8 September 2020; Published: 14 September 2020



Abstract: The absorptance of metals is often low within the visible and near-infrared band at room temperature. Increasing the absorption of metals plays a vital role in reducing energy consumption and production cost. After irradiation by 10 ns linearly polarized pulses with fluence close to the zero-probability damage threshold, the surface of 45# steel samples exhibited four kinds of surface structures in the spot area. The samples' absorptance is improved by 38% when a high-quality laser-induced surface structure (LIPSS) appears at the spot centre. With the increase of the number of pulses, LIPSS begin to melt down, which will decrease the surface absorptance due to the appearance of damage stripes. The relative absorptance of samples was measured by an integrating sphere system. The paper reports detailed experiments to show that LIPSS can improve samples' absorptance significantly.

Keywords: 45# steel; absorptance; LIPSS; laser processing; laser damage

1. Introduction

In 1965, Birnbaum found a series of periodic stripes on semiconductors after irradiation by linearly polarized long pulses generated by a ruby laser [1]. The stripes were later named laser-induced periodic surface structures (LIPSS).

After irradiation near the materials' ablation threshold [2], LIPSS appear on the surface of samples. LIPSS can be observed on nearly all kinds of solid materials, including metals [3], semiconductors [4], crystals [5], ceramic materials [6], polymers [7], etc. Since LIPSS can change the absorptivity [8], hydrophilicity/hydrophobicity [9,10], colourability [11], modulation coding [12], antimicrobial properties [13] and other properties of materials, they have been an interesting research direction for more than half a century.

There are two kinds of LIPSS: low spatial frequency LIPSS (LSFL) and high spatial frequency LIPSS (HSFL). Both types of structure can appear in the same area [14]. The period of LSFL Λ_L and that of HSFL Λ_H can be calculated by the equations below [2,15]:

$$\begin{cases} \Lambda_L = \frac{\lambda}{1 \pm \sin\theta} \\ \Lambda_H = \frac{\lambda}{2\eta} \end{cases}, \quad (1)$$

where λ is the wavelength of the laser, n is the refractive index of the medium, θ is the incident angle, η is the effective refractive index of the materials.

In previous studies, LIPSS on steels were often induced by high-repetition-rate pulses with a focused beam [16–18]. In this paper, LIPSS were produced by 1 Hz pulses. Low-repetition-rate pulses can avoid the influences of thermal effects [19].

Absorptance of targets is a significant index of metals in manufacturing industry laser processing. Typically, within the visible and near-infrared band, the absorptance of metal materials stays at a low level before solid-liquid phase change. Increasing the absorption of metals plays a vital role in reducing energy consumption and production cost. For example, higher absorptance means holes of specific depth can be drilled by pulses with lower energy. There are two ways to realize this: one is raising the temperature of the sample; another one is changing its surface topography.

When irradiated by a normally incident laser, the absorptance A of metal materials with a smooth surface can be calculated approximately by Hagen-Rubens formula [20]:

$$A \approx 2\sqrt{\frac{c}{\lambda_0 \sigma(T)}}, \tag{2}$$

where c is the speed of light, λ_0 is the central wavelength of the laser, σ is the DC conductivity of the material.

DC conductivities of metals reduce when their temperature increases [21]. Therefore, the absorptance of metals can be raised by improving their temperature. However, a higher temperature of materials may lead to lower machining accuracy. Changing the surface topography of samples becomes a better way to promote their absorptance in the precision processing industry. LIPSS, as high-precision microstructures, can improve the absorptance of solid metals significantly [8].

Vorobyev'sgroup reported a series of studies about this [8,22–24]. LIPSS were induced on the surface of gold plates by a femtosecond laser at a centre wavelength of λ = 800 nm, with a pulse duration of τ = 60 fs and repetition rate of f = 1 kHz. The beam was focused by a convex lens. The period of LIPSS was about the wavelength of the laser. The studies were based on the concept of energy deposition, using Equation (2) to calculate the absorption of the samples [8]:

$$A = \frac{C \cdot \Delta T}{N \cdot E_0}, \tag{3}$$

where C is the heat capacity of the metal, ΔT is the increment of the target's temperature, N is the number of pulses, E_0 is the energy of a pulse.

The surface topographies of the samples were observed by a scanning electron microscope (SEM). They found that the absorptance of gold plates was raised when LIPPS appeared.

In this paper, improvements are made based on Vorobyev's works. 45# steel samples were used to find out the relationship between LIPSS and the absorptance of metals. An integrating sphere system was used to measure the absorptance of the samples so any errors caused by heat effects in the measurement of temperature were avoided and the improvement of samples' absorptance only depended on the surface structures. The accuracy of qualitative and quantitative analysis was improved.

Besides, the types of change of samples' surface micromorphology after irradiated were distinguished. The absorptance of samples with different surface micromorphologies was measured in order. The effect of LIPSS and damage stripes could be distinguished. It made the results more rigorous and more comprehensive. What's more, previous works only focused on LSFL. In this paper, both types of LIPSS were studied.

2. Materials and Methods

2.1. Sample Preparation

In order to improve the measurement accuracy of samples' absorptance, the surface of plates should be covered by a large area of LIPSS, so unfocused pulses were used. The sample preparation

system is shown in Figure 1. A Q-switched Nd: YAG laser (SL803, Spectron Lasers, Rugby, UK) was used to generate 10 ns linearly polarized pulses at a central wavelength of 1.064 μm, with a repetition rate of 1 Hz. The maximum energy of a single pulse was 520 mJ. The 8 mm diameter laser beam was narrowed by a 2× beam-reducer. The incident angle was 0°. The pulse energy was adjusted by changing the voltage of the laser's amplifier stage and turning the polarizer. It was monitored online by an energy detector. The polarizer was also used for determining the direction of the laser.

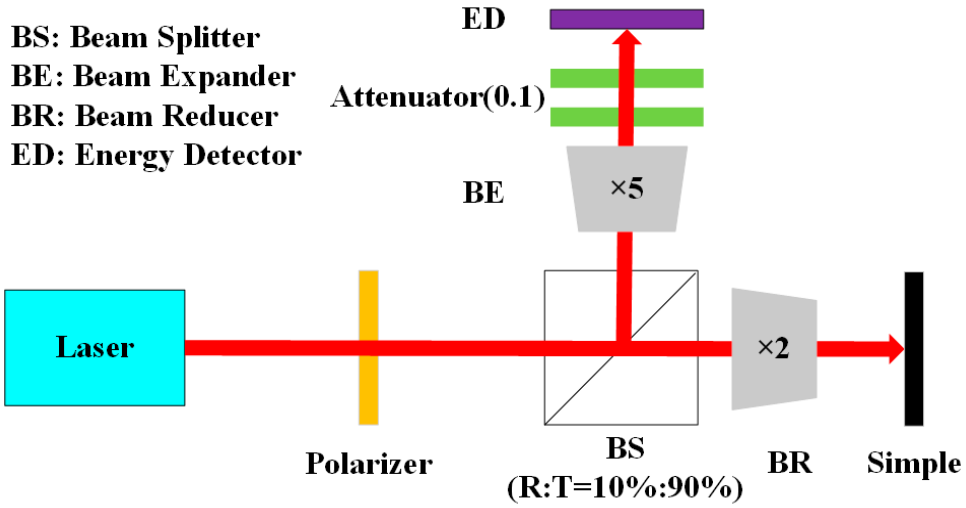


Figure 1. The diagram of the sample preparation system.

45# steel plates with a diameter of 25 mm and a thickness of 5 mm were used in the experiment, as shown in Figure 2. Moreover, their initial average surface roughness is 0.4 μm according to the product manual.

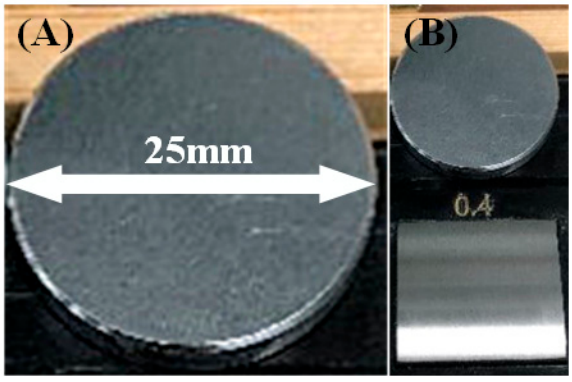


Figure 2. 45# steel samples. (**A**) diameter; (**B**) average surface roughness.

LIPSS are easier to be produced when the polarization direction of the laser is parallel to the polishing direction of samples [25]. Therefore, the direction of polarizer was turned to the direction which was parallel to the scratches.

2.2. Measurement of the Samples' Relative Absorptance

In this paper, the relative absorptance of samples with different morphologies was measured by an integrating sphere system (IS236A, Thorlabs, Munich, Germany). A silicon detector (Thorlabs SM05PD1A) was used. Its response waveband is from 350 nm to 1100 nm, and its output is a current signal. In order to improve the precision of the measurements, samples were put at the port above for avoiding the first reflecting laser from samples to irradiate the detector directly. The probe laser was a continue laser at a central wavelength of 1.064 μm. The measurement system is shown in Figure 3.

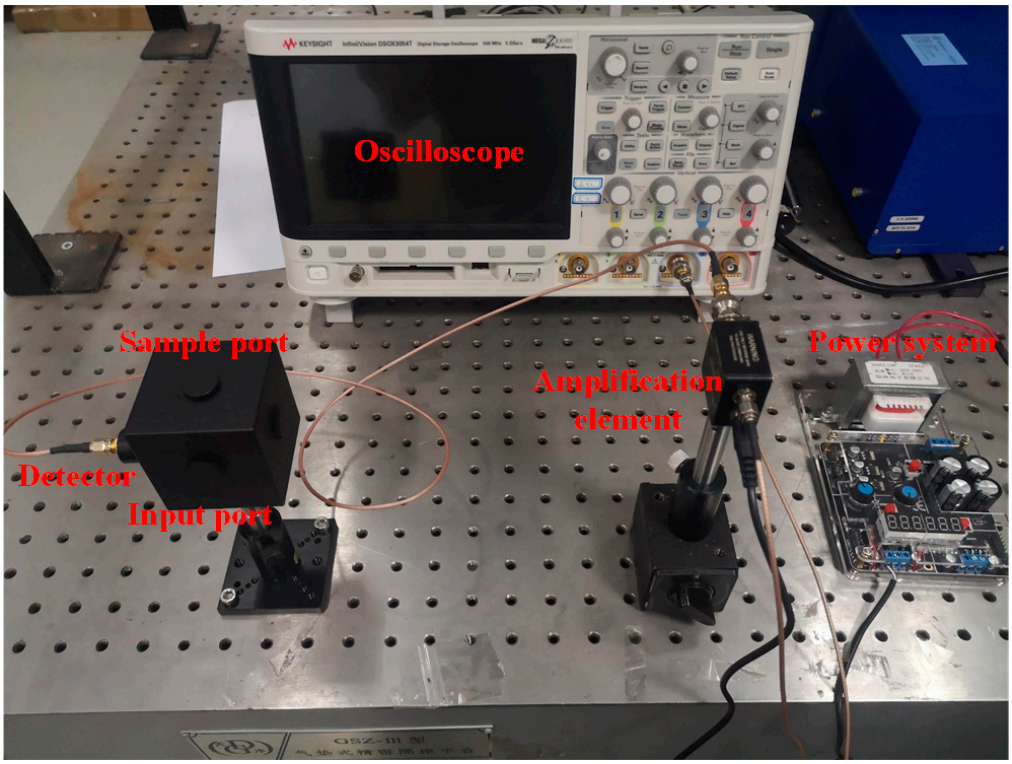


Figure 3. Measurement system.

As the diameter of the sample port was 12.5 mm, about three times larger than that of the laser beam, the measurement results of samples' absorptance were smaller than the actual value. Therefore, the experiment was semi-qualitative and semi-quantitative. 45# steel samples with a smooth surface were set to total reflective samples at the wavelength of 1.064 μm. Then the relative absorptance of samples was measured. The results show the influence of samples' surface microstructures on their absorptance directly. In order to reduce measurement errors caused by the environment, all experiments were carried out in a dark room.

Firstly, the sample port above was opened. Run the probe laser, and the output value was I_b. With the same parameters, a 45# steel sample with a smooth surface was put at the sample port. The output value was I_d. The reflectance of the smooth surface R_d was set to 1. Then the sample under-tested was put at the port, and the real-time indication was I_s. Its relative absorptance A_s could be calculated by Equation (4):

$$A_s = 1 - \frac{I_s - I_b}{I_d - I_b} R_d = 1 - \frac{I_s - I_b}{I_d - I_b}, \quad (4)$$

Because the pulse interval was much longer than the thermal diffusion time of a single pulse, the heat accumulation process of samples could be ignored. Compared with focused beams, the peak fluence of the unfocused beam is lower. Besides, the speed of energy changing from the spot centre to the facula edge is much slower than that of focused beam. Therefore, the surface morphology of the facula edge has influence in the absorptance of samples. It could not be ignored. The surface structures of samples depend on the laser's parameters. In this paper, the influence of the number of pulses and the energy of a single pulse to them was studied.

3. Results

3.1. The Tests of Zero-Probability Damage Threshold of 45# Steel Samples

First of all, the zero-probability damage threshold of the 45# steel samples was tested. 1–on–1 tests are typically used [26]. The measurements were carried out with the number of tested spots was

50. As the results are shown in Figure 4, the zero-probability damage threshold of the samples was $\varphi_0 = 0.957$ J/cm^2, according to the tests.

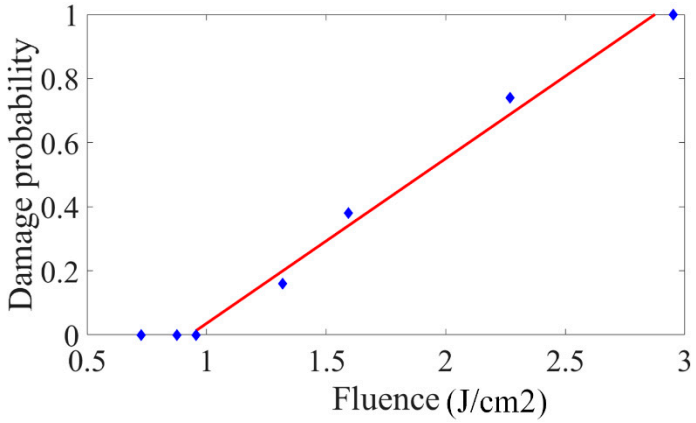


Figure 4. The results of the 1–on–1 tests.

3.2. The Surface Micromorphology of Samples

Then the relationship between the surface micromorphology of the samples and the number of pulses was studied. The fluence of a single pulse was set to $\varphi = 0.955$ J/cm^2, slightly lower than φ_0. The number of pulses N was changed only. A CCD camera was used to take photos of samples' surface micromorphology under an optical microscope.

When N was small, LSFL, whose periods were about 1 μm, only could be seen at the spot centre, shown in Figure 5A–C. LSFL with the direction perpendicular to the polarization direction of the laser were induced by only a few pulses ($N = 25$). As the increased in the number of pulses, the quality of LSFL was becoming better. When $N = 75$, high-quality LSFL could be observed at the spot centre. Then N was raised continually, LSFL at the spot centre began to be destroyed. Meanwhile, LSFL were produced at the facula edge, shown in Figure 5D,E. Figure 5F,G show surface structures when $N = 125$. LSFL at the spot centre were totally destroyed, and HSFL, whose periods were about 0.5 μm, were induced based on LSFL at the facula edge. When $N = 150$, a serious of damage stripes appeared at the spot centre while HSFL at the facula edge were started to be destroyed, shown in Figure 5H,I.

The results above showed that there were four stages of samples' surface structures with the increasing of N: (1) LSFL were induced by the linear-polarization laser at the spot centre; (2) LSFL at the spot centre began to be destroyed while LSFL appeared at the facula edge; (3) LSFL at the spot centre were totally destroyed, and HSFL were induced at the facula edge based on LSFL; (4) Damage stripes could be observed at the spot centre, while HSFL at the facula edge were destroyed.

In the experiments, the quality of LSFL was better than HSFL, and HSFL only appeared at the low-fluence area based on LSFL.

Besides, the influence of a single pulse's energy on the samples' surface micromorphology was studied. As shown in Figure 5C, high-quality LSFL could be observed after irradiated by laser with pulses number $N = 75$ and the fluence of a single pulse $\varphi = 0.955$ J/cm^2. Therefore, N was set to 75. Figure 5 showed the surface micromorphology of the samples with $\varphi = 0.522$ J/cm^2, $\varphi = 0.726$ J/cm^2, $\varphi = 0.955$ J/cm^2, $\varphi = 1.592$ J/cm^2, $\varphi = 2.268$ J/cm^2, $\varphi = 2.952$ J/cm^2 in order.

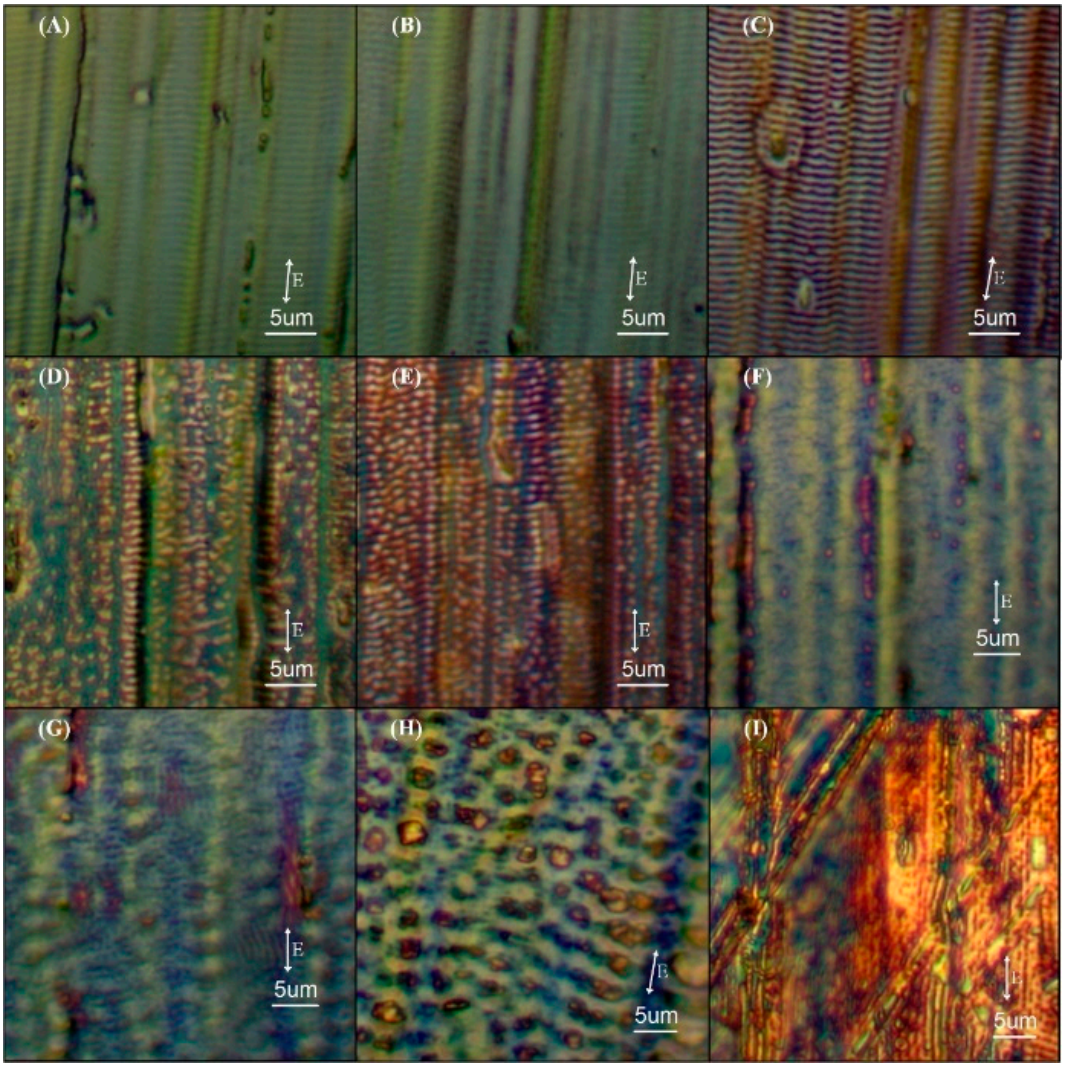


Figure 5. Surface morphology of samples (φ = 0.955 J/cm^2). (**A**)N = 25, the spot centre; (**B**) N = 50, the spot centre; (**C**) N = 75, the spot centre; (**D**) N = 100, the spot centre; (**E**) N = 100, facula edge; (**F**) N = 125, the spot centre; (**G**) N = 125, facula edge; (**H**) N =150, the spot centre; (**I**) N = 150, facula edge.

When φ was too low (φ = 0.522 J/cm^2), only irregular nanoparticles could be observed at the spot centre, is shown in Figure 6A. As the increasing of φ, LSFL appeared at the spot centre. Meanwhile, the quality of LSFL also increased within a range of φ, shown in Figure 6B,C. φ was raised continually, LSFL at the centre of spot area were destroyed, till damage stripes with a period of 5–10 μm appeared at the area (φ = 2.952 J/cm^2). At the same time, LSFL were produced at the facula edge, as shown in Figure 6E,G,I.

A brief conclusion could be obtained from the results above: as the increase of φ, there were four kinds of surface micro-morphologies appeared at the spot centre in order. They were irregular nanoparticles, LSFL, molten LSFL and damage stripes.

What's more, there was only a range of φ could induce LIPSS. When it was too low (φ = 0.522 J/cm^2) or too high (φ = 2.952 J/cm^2), there was no LIPSS appeared at the centre area of the spots.

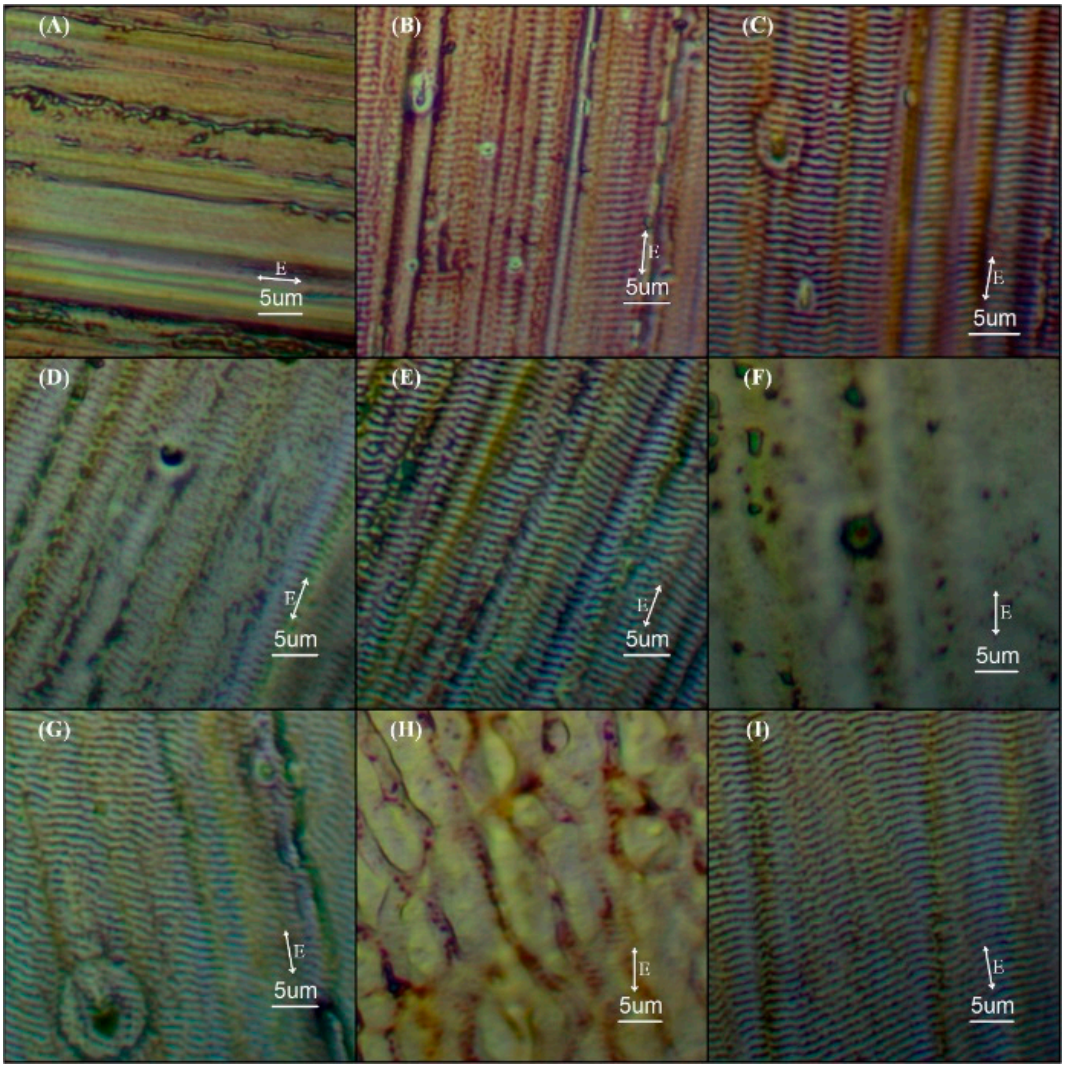


Figure 6. Surface morphology of samples ($N = 75$). (**A**) $\varphi = 0.522$ J/cm^2, the spot centre; (**B**) $\varphi = 0.726$ J/cm^2, the spot centre; (**C**) $\varphi = 0.955$ J/cm^2, the spot centre; (**D**) $\varphi = 1.592$ J/cm^2, the spot centre; (**E**) $\varphi = 1.592$ J/cm^2, facula edge; (**F**) $\varphi = 2.268$ J/cm^2, the spot centre; (**G**) $\varphi = 2.268$ J/cm^2, facula edge; (**H**) $\varphi = 2.952$ J/cm^2, the spot centre; (**I**) $\varphi = 2.952$ J/cm^2, facula edge.

3.3. Relative Absorptance of the Samples

Within the range of energy density that LIPSS could be induced, the fluence gradient of a single pulse was set with four groups ($\varphi = 0.726$ J/cm^2, $\varphi = 0.955$ J/cm^2, $\varphi = 1.592$ J/cm^2, $\varphi = 2.268$ J/cm^2). Each group included six samples, which were irradiated by $N = 25$, $N = 50$, $N = 75$, $N = 100$, $N = 125$, $N = 150$ pulses in order. The integrating sphere system was used to measure the relative absorptance of each sample at a wavelength of 1.064 μm. The results are shown in Figure 7.

The surface structures were observed by an optical microscope. The results showed that the relative absorptance of samples was increased as soon as LSFL appeared at the spot centre. The relative absorptance of the samples improved significantly with the increasing of the area and quantity of LSFL. After LSFL at the spot centre started to be destroyed, the relative absorptance of samples reduced at once, as shown in Figure 7 (N ≥ 100, green line). However, the speed of decreasing was slowed by the production of LSFL at the facula edge, as shown in the red line and green line in Figure 7. The area and quality of LSFL at the facula edge were lower than those at the spot centre. It tended to a constant when LIPSS among the whole area of the spot had been totally destroyed, as shown in the black line in

Figure 7. The value was slightly bigger than that of the relative absorptance of the smooth sample but far smaller than the relative absorptance of samples with high-quality LIPSS.

It could be concluded that both two types of LIPSS, LSFL and HSFL, could improve the absorptance of samples, as shown in the red line and green line in Figure 7. However, HSFL only appeared when φ was low.

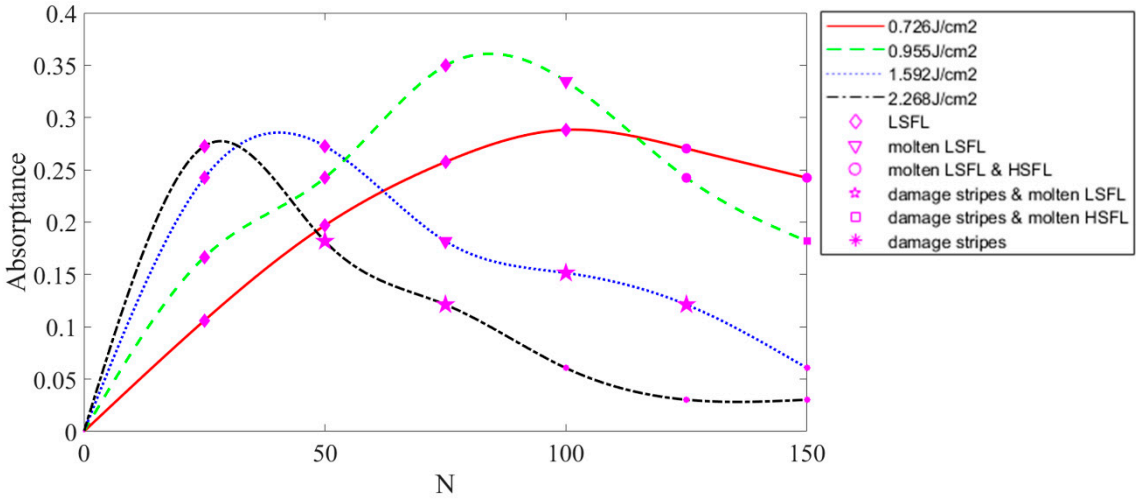


Figure 7. The relative absorptivity of samples.

The result showed that damage stripes also could improve the absorptance of samples, but the degree of improvement was much lower than that of high-quality LIPSS. Only when high-quality LIPSS appeared on the surfaces of the samples, the absorptance enhanced significantly.

4. Discussion

From the experiment results it is clear that LIPSS can improve the absorptance of 45# steel samples. The absorptance of samples with smooth surfaces was gauged accurately by the integrating sphere system. However, as the diameter of laser beam was smaller than that of the sample port, the measurement results of other samples' absorptance were slightly smaller than actual values. That was because the absorptance of samples measured was that of the whole port area, not only the spot area. The improvement of samples' absorptance by surface microstructure was averaged by a large area. Therefore, the measurement of samples' absorptance was a semi-qualitative and semi-quantitative experiment. Thus, the improvement of 45# steel samples' absorptance is better than the results of measurement.

Damage stripes on the surfaces of samples are shown in Figure 5H. The periods of them were about 10 μm so that their spatial frequency was much lower than that of LIPSS. Besides, the directions of damage stripes were irregular. Therefore, damage stripes couldn't modulate the electric field of the incident laser as effective as LIPSS. Hence, the relative absorptance of samples with damage stripes wasn't high.

5. Conclusions

High quality and large area LIPSS are induced on the surface of 45# steel samples by an unfocused beam. The periods of LSFL were about 1 μm while those of HSFL were about 0.5 μm, which was consistent with the conclusion of Equation (1). A linearly polarized pulsed laser at a centre wavelength of λ = 1.064 μm, with a pulse duration of τ = 10 ns and a repetition rate of f = 1 Hz, was used. The relative absorptance of the samples is improved about 38% at the wavelength of 1.064 μm. It is raised significantly no sooner than LIPSS appears. Both types of LIPSS, LSFL and HSFL, can improve the samples' absorptance. The degree of improvement increases with the increase of LIPSS area and

quality. The absorptance of the samples falls as soon as LIPSS at the spot centre begins to be destroyed. After the samples are totally damaged, their relative absorptance decrease to 0.03, slightly more than that of the smooth sample. Therefore, it is LIPSS that improved the absorptance of samples significantly.

Author Contributions: Conceptualization, T.W. and X.L.; methodology, resource and project administration, J.B.; software, data curation and funding acquisition, X.L.; validation, H.K., L.W. and X.W.; formal analysis, X.S.; investigation and writing—original draft preparation, T.W.; writing—review and editing, X.L. and J.B.; visualization, X.W.; supervision, J.B. and X.S. All authors have read and agreed to the published version of the manuscript.

Funding: This research was funded by the Anhui Province Natural Science Foundation (Project No.1908085MF222), the research was supported by Anhui Natural Science Foundation of Youth Fund Project (Project No.2008085QF314), Advanced Laser Technology Anhui Laboratory Youth Fund Project (Project No.ky19c604), and Projects of National University of Defense Technology (Project No.zk19-15), and Foundation of the State Key Laboratory of Pulsed Power Laser Technology (Project No.SKL2019ZR04).

Acknowledgments: The authors acknowledge the support from funds.

Conflicts of Interest: The authors declare no conflict of interest. The funders had no role in the design of the study; in the collection, analyses, or interpretation of data; in the writing of the manuscript, or in the decision to publish the results.

References

1. Birnbaum, M. Semiconductor Surface Damage Produced by Ruby Lasers. *J. Appl. Phys.* **1965**, *36*, 3688. [CrossRef]
2. Graef, S.; Mueller, F.A. Polarisation-dependent generation of fs-laser induced periodic surface structures. *Appl. Surf. Sci.* **2015**, *331*, 150–155. [CrossRef]
3. Golosov, E.V.; Ionin, A.A.; Kolobov, Y.R.; Kudryashov, S.; Ligachev, A.E.; Makarov, S.V.; Novoselov, Y.N.; Seleznev, L.V.; Sinitsyn, D.V. Formation of periodic nanostructures on aluminum surface by femtosecond laser pulses. *Nanotechnol. Russ.* **2011**, *6*, 237–243. [CrossRef]
4. Bonse, J.; Baudach, S.; Krüger, J.; Kautek, W.; Lenzner, M. Femtosecond laser ablation of silicon-modification thresholds and morphology. *Appl. Phys. A* **2002**, *74*, 19–25. [CrossRef]
5. Shao, J.; Liang, X.; You, L.; Pan, N.; Lin, Y.; Wang, S.; Deng, Z.; Fang, X.; Wang, X. Laser-induced damage and periodic stripe structures of a CaF2 single crystal by an ArF excimer laser. *Chin. Opt. Lett.* **2020**, *18*, 021403. [CrossRef]
6. Dumitru, G.; Romano, V.; Weber, H.P.; Sentis, M.; Marine, W. Ablation of carbide materials with femtosecond pulses. *Appl. Surf. Sci.* **2003**, *205*, 80–85. [CrossRef]
7. Baudach, S.; Bonse, J.; Kautek, W. Ablation experiments on polyimide with femtosecond laser pulses. *Appl. Phys. A* **1999**, *69*, S395–S398. [CrossRef]
8. Vorobyev, A.Y.; Guo, C. Enhanced absorptance of gold following multipulse femtosecond laser ablation. *Phys. Rev. B* **2005**, *72*, 195422. [CrossRef]
9. Vorobyev, A.Y.; Guo, C. Laser turns silicon superwicking. *Opt. Express* **2010**, *18*, 6455–6460. [CrossRef]
10. Barberoglou, M.; Zorba, V.; Stratakis, E.; Spanakis, E.; Tzanétakis, P.; Anastasiadis, S.H.; Fotakis, C. Bio-inspired water repellent surfaces produced by ultrafast laser structuring of silicon. *Appl. Surf. Sci.* **2009**, *255*, 5425–5429. [CrossRef]
11. Dusser, B.; Sagan, Z.; Soder, H.; Faure, N.; Colombier, J.; Jourlin, M.; Audouard, E. Controlled nanostructrures formation by ultra fast laser pulses for color marking. *Opt. Express* **2010**, *18*, 2913–2924. [CrossRef] [PubMed]
12. Landon, S. Micro-et Nano-Usinage par Laser à Impulsions Ultracourtes: Amélioration de Procédés par des Méthodes Tout Optique. 2011. Available online: https://tel.archives-ouvertes.fr/tel-00719223/ (accessed on 20 October 2012).
13. Ivanova, E.P.; Hasan, J.; Webb, H.K.; Gervinskas, G.; Juodkazis, S.; Truong, V.K.; Wu, A.H.; Lamb, R.N.; Baulin, V.A.; Watson, G.S.; et al. Bactericidal activity of black silicon. *Nat. Commun.* **2013**, *4*, 2838. [CrossRef] [PubMed]
14. Gregorčič, P.; Sedlaček, M.; Podgornik, B.; Reif, J. Formation of laser-induced periodic surface structures (LIPSS) on tool steel by multiple picosecond laser pulses of different polarizations. *Appl. Surf. Sci.* **2016**, *387*, 698–706. [CrossRef]

15. Zhiming, L.; Xi, W.; Jinsong, N.; Yuze, H. High frequency femtosecond laser induced periodic spatial structure on silicon surface. *Infrared Laser Eng.* **2018**, *47*, 0106003. [CrossRef]
16. Hu, Y.; Fan, N.; Lu, Y.; Sun, X.; Wang, C.; Xia, Z.; Duan, J.; Wang, H.; Zhou, J.; Luo, Z.; et al. LIPSS formed on the sidewalls of microholes in stainless steel trepanned by a circularly polarized femtosecond laser. *Appl. Phys. A* **2016**, *122*, 665. [CrossRef]
17. Hikage, H.; Nosaka, N.; Matsuo, S. High-spatial-frequency periodic surface structures on steel substrate induced by subnan osecond laser pulses. *Appl. Phys. Express* **2017**, *10*, 112701. [CrossRef]
18. Simões, J.; Riva, R.; Miyakawa, W. High-speed Laser-Induced Periodic Surface Structures (LIPSS) generation on stainless steel surface using a nanosecond pulsed laser. *Surf. Coat. Technol.* **2018**, *344*, 423–432. [CrossRef]
19. Pozdnyak, N.Z. Review of book by V. E. Mikryukov "thermal and electrical conductivity of metals and alloys". *Met. Sci. Heat Treat.* **1960**, *2*, 636–637. [CrossRef]
20. Prokhorov, A.M.; Konov, V.I.; Ursu, I.; Mihailescu, I.N. *Heating of Metals*; CRC Press: Boca Raton, FL, USA, 1991; pp. 279–280.
21. Di Niso, F.; Gaudiuso, C.; Sibillano, T.; Mezzapesa, F.P.; Ancona, A.; Lugarà, P.M. Role of heat accumulation on the incubation effect in multi-shot laser ablation of stainless steel at high repetition rates. *Opt. Express* **2014**, *22*, 12200–12210. [CrossRef]
22. Vorobyev, A.; Guo, C.; Makin, V.; Kokody, N.; Kuzmichev, V. Effect of surface structural modification on absorptivity of gold in multi-pulse femtosecond laser ablation. In Proceedings of the CAOL 2005. Second International Conference on Advanced Optoelectronics and Lasers, Yalta, Crimea, Ukraine, 12–17 September 2005.
23. Vorobyev, A.Y.; Guo, C. Change in absorptance of metals following multi-pulse femtosecond laser ablation. *J. Phys. Conf. Ser.* **2007**, *59*, 579–584. [CrossRef]
24. Vorobyev, A.Y.; Guo, C.; Makin, V.S.; Kokody, N.G.; Kuzmichev, V.M. Extraordinary enhanced absorptivity of gold surface ablated with femtosecond laser pulses. *SPIE Proc.* **2008**, *7009*, 700913. [CrossRef]
25. Ardron, M.; Weston, N.; Hand, D.; Weston, N. A practical technique for the generation of highly uniform LIPSS. *Appl. Surf. Sci.* **2014**, *313*, 123–131. [CrossRef]
26. Liu, X.; Li, D.; Zhao, Y.A.; Li, X.; Ling, X.; Shao, J. Damage characteristics of HfO_2/SiO_2 high reflector at 45° incidence in 1-on-1 and N-on-1 tests. *Chin. Opt. Lett.* **2010**, *8*, 41–44.



© 2020 by the authors. Licensee MDPI, Basel, Switzerland. This article is an open access article distributed under the terms and conditions of the Creative Commons Attribution (CC BY) license (http://creativecommons.org/licenses/by/4.0/).